FES Cycling in Stroke: Novel Closed-Loop Algorithm Accommodates Differences in Functional Impairments

Courtney A. Rouse [ID], Ryan J. Downey, Chris M. Gregory, Christian A. Cousin [ID], Victor H. Duenas [ID], and Warren E. Dixon [ID]

Abstract*—*Objective: **The objective of this paper was to develop and test a novel control algorithm that enables stroke survivors to pedal a cycle in a desired cadence range despite varying levels of functional abilities after stroke. *Methods:* A novel algorithm was developed which automatically adjusts 1) the intensity of functional electrical stimulation (FES) delivered to the leg muscles, and 2) the current delivered to an electric motor. The algorithm automatically switches between assistive, uncontrolled, and resistive modes to accommodate for differences in functional impairment, based on the mismatch between the desired and actual cadence. Lyapunov-based methods were used to theoretically prove that the rider's cadence converges to the desired cadence range. To demonstrate the controller's real-world performance, nine chronic stroke survivors performed two cycling trials: 1) volitional effort only and 2) volitional effort accompanied by the control algorithm assisting and resisting pedaling as needed. *Results:* With a desired cadence range of 50–55 r/min, the developed controller resulted in an average rms cadence error of 1.90 r/min, compared to 6.16 r/min during volitional-only trials. *Conclusion:* Using FES and an electric motor with a two-sided cadence control objective to assist and resist volitional efforts enabled stroke patients with varying strength and abilities to pedal within a desired cadence range. *Significance:* A protocol design that constrains volitional movements with assistance and resistance from FES and a motor shows potential for FES cycles and other rehabilitation robots during stroke rehabilitation.**

***Index Terms*—Nonlinear control systems, rehabilitation robotics switching systems.**

I. INTRODUCTION

THERE are nearly 7 million stroke survivors in the United States; however, according to the National Stroke Association, stroke recovery is a lifelong process and warrants

safe, convenient, and noninvasive treatment protocols for rehabilitation. Functional electrical stimulation (FES) is commonly used to artificially induce coordinated functional movements in people with lower limb movement disorders (e.g., post-stroke). FES has been shown to impart health benefits such as improving muscle strength [1], range of motion [2], spasticity [3], and blood glucose and insulin levels [4]. Furthermore, coordinating the activation of multiple lower body muscle groups with cycling is a beneficial rehabilitation exercise [5]–[13] that may outperform therapy with isometric FES contractions [14]. Specifically, FES-cycling may improve bone mineral density [15], [16]; physiological motor control [17]; cardiovascular parameters [16], [18]; muscle strength and volume [16], [17]; combined motor-sensory scores [19]; and walking speed and spasticity [20] in people with various neuromuscular disorders.

Compared to purely volitional cycling, a combination of FES-cycling and volitional contribution (i.e., FES-assisted cycling) resulted in greater improvements in cadence, power output, heart rate, and performance variability in people with cerebral palsy [21]. Therefore, motivation exists to enable protocols for rehabilitative cycling integrating volition with closed-loop FES-cycling methods. The overwhelming majority of individuals following injury or disease of the central nervous system have some degree of motor and sensory sparing (e.g., stroke patients). As such, developing globally effective rehabilitation tools will require the ability to accommodate patients across a wide range of volitional capabilities. Moreover, since the goal of rehabilitation is to restore volitional function, the participants are encouraged to volitionally pedal during the cycling protocol, rather than remain passive, as in [22]. Motivated by the desire to combine FES-induced cycling and an electric motor to minimally constrain and assist a volitionally pedaling rider, we develop a new cycling strategy that constrains the rider's cadence within an upper and lower cadence threshold.

Motivated by the large variation of strength and abilities among people requiring physical therapy, a closed-loop control method is developed in this paper to yield a desired cadence, despite uncertainty in the participant's abilities. The closed-loop system contributes to the cadence goal, but only when the user fails to meet the desired cadence range. Some controllers for rehabilitation robots have been developed that constrain the states to a desired range. For instance, in [23], an assist-as-needed
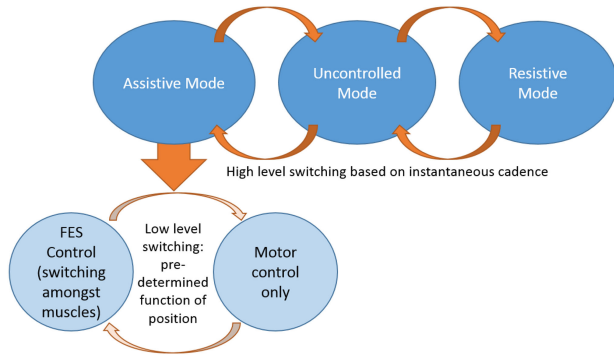
Fig. 1. Diagram illustrating the combined two-level switched system.

control algorithm for a motorized wrist system restricts volitional arm movements, but only when outside of a changing allowable error range. Similarly, virtual fixtures have been used to limit range of motion during vision-assisted control [24] and force fields have been used for many robotic applications (e.g., surgical robotics [25], [26]). Control algorithms to limit robotic assistance have been implemented for post-stroke rehabilitation protocols, both with FES [27], [28] and without FES [29], [30]. However, the idea of constraining voluntary motion within state boundaries has not yet been extended to FES-cycling protocols and unlike the mentioned studies, the system in this paper is constrained by cadence rather than force. Moreover, system stability that accounts for switching amongst multiple actuators is proven via Lyapunov methods in the appendix.

In this paper, a closed-loop state-dependent switched system operates within three modes (3Ms): assistive, uncontrolled (i.e., only volitional contribution), and resistive, each based on real-time cadence feedback in comparison to thresholds that make up a desired cadence range, selected a priori by the user or a physical therapist. FES is applied to assist the rider when the cycling cadence is below the minimum threshold; however, since there exist kinematically inefficient regions of the crank cycle (i.e., leg positions that require large muscle forces to produce comparatively low torque about the crank [12], [31]–[33]), a low level of switching within the assistive mode occurs between FES and the electric motor, both of which are stable subsystems. Specifically, switching occurs when activating different combinations of lower limb muscle groups to coordinate the limb trajectories through FES regions (kinematically efficient regions) and the motor regions (kinematically inefficient regions). If the rider is able to volitionally pedal between the minimum and maximum desired cadences then the system switches to the uncontrolled (but bounded) mode where no control input is sent to either the motor or FES. If the rider's volitional efforts exceed the upper cadence threshold, then switching will transition the cycle-rider system from the uncontrolled mode to the resistive mode, where the motor will engage to provide resistive torques to push the rider back into the desired cadence range. In addition to the benefits of resistance training for stroke survivors [34], an upper threshold on the desired cadence range also has the benefit of bounding the uncontrolled mode for stability purposes. Figure 1 depicts the multi-level combined switched system.

As in the preliminary results in [35], Lyapunov-based methods for switched systems are used to examine the stability of the family of sliding mode controllers. A common Lyapunov function with a set-valued generalized derivative is used to prove stability, despite uncertain rider dynamics, pedaling abilities, or bounded disturbances, provided sufficient gain conditions are satisfied. Global exponential stability is achieved for the controllers operating in the assistive and resistive modes, and the trajectories in the volitional only mode are bounded above and below by the controlled subsystems at the upper and lower cadence thresholds. The work in this paper builds upon the precursory mathematical stability analysis in [35] with experimental validation using stroke survivors since they have been shown to benefit from FES-cycling [36] and can generally contribute volitionally. Stroke patients display significant asymmetries and range of abilities depending on the initial stroke severity and subsequent recovery; however, controller performance is confirmed with experimental results on nine stroke patients that illustrate all three cycling modes across a desired cadence range of 50–55 RPM. The desired range of 50–55 RPM was selected for the current experiments as a range of values that is typical of FES-cycling in the stroke population [37].

II. MODEL

The combined cycle-rider dynamics are modeled as[1][33]

$$\tau_e(t) = \tau_c(\dot{q}, \ddot{q}, t) + \tau_r(q, \dot{q}, \ddot{q}, t), \qquad (1)$$

where $q : \mathbb{R}_{\geq 0} \to \mathcal{Q}$ denotes the measurable crank angle and $\mathcal{Q} \subseteq \mathbb{R}$ denotes the set of all crank angles contained between $[0, 2\pi)$. Torques applied about the crank axis by the cycle and the rider are denoted by $\tau_c : \mathbb{R} \times \mathbb{R} \times \mathbb{R}_{\geq 0} \to \mathbb{R}$ and $\tau_r : \mathcal{Q} \times \mathbb{R} \times \mathbb{R} \times \mathbb{R}_{\geq 0} \to \mathbb{R}$, respectively. The torque applied about the crank axis by the electric motor, $\tau_e : \mathbb{R}_{\geq 0} \to \mathbb{R}$, is

$$\tau_e(t) = B_e u_e(t), \qquad (2)$$

where the unknown motor control constant, $B_e \in \mathbb{R}_{>0}$, relates the motor's input current to output torque, and $u_e : \mathbb{R}_{\geq 0} \to \mathbb{R}$ is the subsequently designed motor control current input. The cycle and rider torques, τ_c and τ_r, are defined as

$$\tau_c(\dot{q}, \ddot{q}, t) \triangleq J_c \ddot{q} + b_c \dot{q} + d_c(t), \qquad (3)$$

$$\tau_r(q, \dot{q}, \ddot{q}, t) \triangleq \tau_p(q, \dot{q}, \ddot{q}) - \tau_M(q, \dot{q}, t) + d_r(t), \qquad (4)$$

respectively, where $J_c \in \mathbb{R}_{>0}$, $b_c \in \mathbb{R}_{>0}$, and $d_c : \mathbb{R}_{\geq 0} \to \mathbb{R}$ denote inertial effects, viscous damping effects, and disturbances applied by the cycle, respectively, and $\tau_p : \mathcal{Q} \times \mathbb{R} \times \mathbb{R} \to \mathbb{R}$, $\tau_M : \mathcal{Q} \times \mathbb{R} \times \mathbb{R}_{\geq 0} \to \mathbb{R}$, and $d_r : \mathbb{R}_{\geq 0} \to \mathbb{R}$ denote the passive torques by the rider, the combination of volitional and FES induced muscle contribution, and the rider's disturbances (e.g., spasticity or changes in load), respectively. The passive torques applied by the rider are further divided as

$$\tau_p(q, \dot{q}, \ddot{q}) \triangleq M_p(q)\ddot{q} + V(q, \dot{q})\dot{q} + G(q) + P(q, \dot{q}), \quad (5)$$

---

[1]For notational brevity, all explicit dependence on time, t, within the terms $q(t)$, $\dot{q}(t)$, $\ddot{q}(t)$ is suppressed.

where $M_p : \mathcal{Q} \to \mathbb{R}_{>0}$, $V : \mathcal{Q} \times \mathbb{R} \to \mathbb{R}$, $G : \mathcal{Q} \to \mathbb{R}$, and $P : \mathcal{Q} \times \mathbb{R} \to \mathbb{R}$ denote the inertial, centripetal-Coriolis, gravitational, and passive viscoelastic tissue forces, respectively. The torques applied by the muscles can be separated into volitional contributions and the sum of each muscle's individual contribution by FES as

$$\tau_M (q, \dot{q}, t) \triangleq \sum_{m \in \mathcal{M}} B_m (q, \dot{q}) u_m (t) + \tau_{vol} (t), \qquad (6)$$

$\forall m \in \mathcal{M}$, where $u_m : \mathbb{R}_{\geq 0} \to \mathbb{R}$ is the subsequently designed muscle control current input, and the subscript $m \in \mathcal{M} = \{RQ, LQ\}$ indicates the right (R) and left (L) quadriceps femoris (Q) muscle groups, respectively. The rider's volitional torque is denoted by $\tau_{vol} \in \mathbb{R}_{\geq 0}$. The uncertain individual muscle control effectiveness is denoted by $B_m : \mathcal{Q} \times \mathbb{R} \to \mathbb{R}_{>0}$, $\forall m \in \mathcal{M}$. Definitions for the subsequent FES regions and switching laws during the assistive mode are based on [12], where each particular muscle group is stimulated at specific portions of the crank cycle (i.e., when kinematically efficient) denoted by $\mathcal{Q}_m \subset \mathcal{Q}$. In this manner, $\mathcal{Q}_m$ is defined for each muscle group as

$$\mathcal{Q}_m \triangleq \{q \in \mathcal{Q} \mid T_m (q) > \varepsilon_m\}, \qquad (7)$$

$\forall m \in \mathcal{M}$, where $\varepsilon_m \in (0, \max(T_m)]$ is the lower threshold for each torque transfer ratio, which limits the FES regions for each muscle so that each muscle group can only contribute to forward pedaling (i.e., positive crank motion). Based on the FES regions defined in (7), let $\sigma_m (q) \in \{0, 1\}$ be a piecewise left-continuous switching signal for each muscle group such that $\sigma_m (q) = 1$ when $q \in \mathcal{Q}_m$ and $\sigma_m (q) = 0$ when $q \notin \mathcal{Q}_m$, $\forall m \in \mathcal{M}$. The union of FES regions, denoted by $\mathcal{Q}_{FES}$, is defined as $\mathcal{Q}_{FES} \triangleq \underset{m \in \mathcal{M}}{\cup} \{\mathcal{Q}_m\}, \forall m \in \mathcal{M}$.

Within the assistive mode, position-based switching is used to switch between subsets of muscle groups and the motor. When switching between assistive, uncontrolled, and resistive modes, the switching velocity (i.e., cadence) values $\{\dot{q}_{\underline{d}} : \mathbb{R}_{\geq 0} \to \mathbb{R}_{>0}, \dot{q}_{\overline{d}} : \mathbb{R}_{\geq 0} \to \mathbb{R}_{>0}\}$ are known but the position values at which they occur are not. To facilitate the analysis of a combination of position-based switching (within the assistive mode) and velocity-based switching (amongst the 3Ms), switching times are denoted by $\{t_n^i\}, i \in \{s, e, p\}, n \in \{0, 1, 2, \ldots\}$, representing the times when the crank transitions into the FES region when in assistive mode (s), an electric motor region $(e$, either assistive or resistive$)$, or neither $(p$, i.e., uncontrolled mode$)$.

In (6), the electrical stimulation intensity input (i.e., pulsewidth) to each individual muscle is denoted by $u_m : \mathbb{R}_{\geq 0} \to \mathbb{R}$, and defined as

$$u_m \triangleq \sigma_m k_m u_s (t), \qquad (8)$$

$\forall m \in \mathcal{M}$, where $u_s : \mathbb{R}_{\geq 0} \to \mathbb{R}$ denotes the subsequently designed FES control input and $k_m \in \mathbb{R}_{>0}$ is a constant control gain. Substituting (2)-(6) and (8) into (1) yields[2]

$$B_M u_s + B_e u_e + \tau_{vol}$$
$$= M\ddot{q} + b_c \dot{q} + d_c + V\dot{q} + G + P + d_r, \qquad (9)$$

where $M : \mathcal{Q} \to \mathbb{R}$ is defined as the summation $M \triangleq J_c + M_p$, and $B_M : \mathcal{Q} \times \mathbb{R} \to \mathbb{R}$ is the combined switched FES control effectiveness, defined as

$$B_M (q, \dot{q}) \triangleq \sum_{m \in \mathcal{M}} B_m \sigma_m k_m. \qquad (10)$$

The switched system in (9) has the following properties and assumptions:

Property: 1 $c_m \leq M \leq c_M$, where $c_m, c_M \in \mathbb{R}_{>0}$ are known constants. **Property: 2** $|V| \leq c_V |\dot{q}|$, where $c_V \in \mathbb{R}_{>0}$ is a known constant and $|\cdot|$ denotes absolute value. **Property: 3** $|G| \leq c_G$, where $c_G \in \mathbb{R}_{>0}$ is a known constant. **Property: 4** $|P| \leq c_{P1} + c_{P2}|\dot{q}|$, where $c_{P1}, c_{P2} \in \mathbb{R}_{>0}$ are known constants. **Property: 5** $b_{c_l} \dot{q}_l \leq c_b |\dot{q}_l|$, where $c_b \in \mathbb{R}_{>0}$ is a known constant. **Property: 6** $|d_r + d_c| \leq c_d$, where $c_d \in \mathbb{R}_{>0}$ is a known constant [31]. **Property: 7** $\frac{1}{2}\dot{M} = V$. **Property: 8** The muscle control effectiveness B_m is lower bounded $\forall m \in \mathcal{M}$, and thus, when $\sum_{m \in \mathcal{M}} \sigma_m > 0$, $c_{b_M} \leq B_M$, where $c_{b_M} \in \mathbb{R}_{>0}$ [12]. **Property: 9** $c_{b_e} \leq B_e \leq c_{B_e}$, where $c_{b_e}, c_{B_e} \in \mathbb{R}_{>0}$. **Assumption: 1** The volitional torque produced by the participant is bounded, due to human physical limitations, as $|\tau_{vol}| \leq c_{vol}$, where $c_{vol} \in \mathbb{R}_{>0}$.

III. CONTROL DEVELOPMENT

The cadence tracking objective is quantified by the cadence error $e_1 : \mathbb{R}_{\geq 0} \to \mathbb{R}$ and an auxiliary error $e_2 : \mathbb{R}_{\geq 0} \to \mathbb{R}$, defined as

$$e_1 (t) \triangleq \dot{q}_{\underline{d}} (t) - \dot{q} (t), \qquad (11)$$

$$e_2 (t) \triangleq e_1 (t) + (1 - \sigma_a (t)) \Delta_d, \qquad (12)$$

where $\dot{q}_{\underline{d}}$ and $\dot{q}_{\overline{d}}$, defined previously, are related as $\dot{q}_{\overline{d}} = \dot{q}_{\underline{d}} + \Delta_d$, where $\Delta_d \in \mathbb{R}_{>0}$ is the size of the desired cadence range. The switching signal that activates the assistive mode $\sigma_a : \mathbb{R}_{\geq 0} \to \{0, 1\}$ is designed as

$$\sigma_a \triangleq \begin{cases} 1 & \text{if } \dot{q} < \dot{q}_{\underline{d}} \\ 0 & \text{if } \dot{q} \geq \dot{q}_{\underline{d}} \end{cases}. \qquad (13)$$

Note that by (12), when $\sigma_a = 1, e_1 = e_2$. Taking the time derivative of (11), multiplying by M, and using (9) and (11) yields

$$M\dot{e}_1 = -B_e u_e - B_M u_s - \tau_{vol} - V e_1 + \chi, \qquad (14)$$

where the auxiliary term $\chi : \mathcal{Q} \times \mathbb{R} \times \mathbb{R}_{\geq 0} \to \mathbb{R}$ is defined as

$$\chi \triangleq b_c \dot{q} + d_c + G + P + d_r + V\dot{q}_{\underline{d}} + M\ddot{q}_{\underline{d}}.$$

From Properties 1–6, χ can be bounded as

$$\chi \leq c_1 + c_2 |e_1|, \qquad (15)$$

---

[2]For notational brevity, all functional dependencies are hereafter suppressed unless required for clarity of exposition.

TABLE I
PARTICIPANT DESCRIPTION

Participant	1	2	3	4	5	6	7	8	9
Age	24	55	49	61	72	48	67	65	36
Sex	M	F	M	M	M	F	F	M	M
Affected Side	R	L	R	R	R	R	L	L	L
Time since Stroke (months)	87	36	25	35	72	42	76	38	172
Self Selected Walking Speed (cm/s)	115.5	92.2	125.8	109.0	61.7	116.4	52.1	134.8	53.4
Fastest Comfortable Walking Speed (cm/s)	154.5	117.5	141.1	155.5	90.4	178.9	77.4	200.0	90.4

where c_1, $c_2 \in \mathbb{R}_{>0}$ are known constants. As in [35] and based on (14), (15), and the stability analysis provided in the appendix, the FES control input to the muscle is designed as

$$u_s = \sigma_a \left(k_{1s} + k_{2s} e_1\right), \quad (16)$$

where k_{1s}, $k_{2s} \in \mathbb{R}_{>0}$ are constant control gains and σ_a is defined in (13). The switched control input to the motor is designed as

$$u_e = \sigma_e \left(k_{1e} \operatorname{sgn}\left(e_1\right) + k_{2e} e_2\right), \quad (17)$$

where k_{1e}, $k_{2e} \in \mathbb{R}_{>0}$ are constant control gains and $\sigma_e : \mathbb{R}_{\geq 0} \to \mathbb{R}_{\geq 0}$ is the motor's switching signal, designed as

$$\sigma_e \triangleq \begin{cases} k_a & \text{if } \dot{q} < \dot{q}_{\underline{d}},\ q \notin Q_{FES} \\ 0 & \text{if } \dot{q} < \dot{q}_{\underline{d}},\ q \in Q_{FES} \\ 0 & \text{if } \dot{q}_{\underline{d}} \leq \dot{q} \leq \dot{q}_{\overline{d}} \\ k_r & \text{if } \dot{q} > \dot{q}_{\overline{d}} \end{cases}, \quad (18)$$

where k_a, $k_r \in \mathbb{R}_{>0}$ are constant control gains. Substituting (16) and (17) into (14) yields

$$M \dot{e}_1 = -B_e \sigma_e \left(k_{1e} \operatorname{sgn}\left(e_1\right) + k_{2e} e_2\right)$$
$$- B_M \sigma_a \left(k_{1s} + k_{2s} e_1\right) - \tau_{vol} - V e_1 + \chi. \quad (19)$$

The stability analysis which proves global exponential tracking to the desired cadence range is provided in the appendix.

IV. EXPERIMENTS

To evaluate the performance of the FES and motor controllers in (16) and (17), respectively, experiments were conducted on nine stroke participants, five affected on their right side and four on their left side, after they gave written informed consent approved by the Medical University of South Carolina Institutional Review Board, with process number Pro00075399. Self-selected and fastest comfortable walking speeds (SSWS and FCWS, respectively) were measured via an instrumented walkway (GAITRite Classic, CIR Systems) before conducting each FES-cycling experiment, and are reported in Table I as an indicator of each individual's walking impairment following stroke.

A. Experimental Setup

A commercially available recumbent tricycle (TerraTrike Rover X8) was modified similar to [12] by adding a 24 VDC electric motor (MY1016Z2, Unite Motor Co. Ltd.) to the drive chain; fixing orthotic boots to the pedals (Rebound Air Walker, Össur Americas); placing the front wheels on riser rings (Kinetic by Kurt); and attaching the rear wheel/axel to a stationary cycling trainer (Kinetic Magnetic 3.0 Trainer, Kinetic by Kurt) that provides adjustable resistance. A servo drive (AB25A100 Ax-Cent, Advanced Motion Controls) was used to control the electric motor, powered by a 300 W, 24 VDC supply (PS300W24, Advanced Motion Controls); and a 95 W, 50 VDC shunt regulator was used to clamp the supply voltage during regeneration (SRST50, Advanced Motion Controls).

Participants were comfortably seated with their feet secured to the cycle in the orthotic boots, preventing ankle plantar-/dorsiflexion and maintaining sagittal alignment of the legs. The seat was adjusted to prevent knee hyper-extension, and measurements of the lower limbs of each participant's legs were taken to calculate the switching points for stimulation and motor activation within the assistive mode, as in [12]. An optical encoder (US Digital H1) was used to measure the crank position and velocity. Data acquisition hardware (Quanser Q8-USB) measured the encoder input and an analog voltage output was used to command the servo drive to deliver the desired current to the electric motor. Both the motor and FES controllers were implemented on a computer running real-time control software (QUARC, MATLAB/Simulink, Windows 10) at a sampling rate of 500 Hz. Electrodes were placed over the participant's left and right quadriceps femoris muscle groups according to Axelgaard's electrode placement manual.[3] Symmetric rectangular biphasic pulses were delivered to the participant's muscle groups with a current-controlled stimulator (Hasomed RehaStim) via self-adhesive electrodes. The stimulation amplitudes were fixed at 40 mA. Stimulation frequency was fixed at 35 Hz. The stimulation pulse width for each muscle group was determined by u_m and u_s from (8) and (16), respectfully, and commanded to the stimulator by the control software. For safety, an emergency stop switch was connected to the data aquisition device to simultaneously stop the electric motor and FES on command.

---

[3]http://www.palsclinicalsupport.com/videoElements/videoPage.php

TABLE II
CYCLING METRICS FROM NINE STROKE PARTICIPANTS

Metric	Seg.	Cond.	Mean	p-value	Participant Number								
					1	2	3	4	5	6	7	8	9
Avg. Cad. (RPM)	OA	Vol	51.54	0.5553	50.96	48.65#	55.51	53.60	49.80^	53.67	47.35^	59.26	45.08^
		3M	51.01		51.86^	48.22	54.67	51.81	49.16^	53.48	49.40^	52.88^	47.60^
	F240	Vol	49.91	0.1434	50.68	48.95	52.42	51.47	49.80^	52.10	47.35^	52.07	44.39
		3M	50.67		51.81	47.76	53.78	50.73	49.13	53.14	49.34	52.86	47.49
	FP	Vol	62.34	0.1201	52.08	47.23#	67.87	61.13	-	59.93	-	88.03	60.16^
		3M	53.99		55.39^	50.05	58.23	56.13	50.25^	54.82	49.81^	59.84^	51.37^
Cad. SD (RPM)	F240	Vol	4.61	0.0223*	2.68	4.38	2.07	2.02	5.79^	2.35	7.70^	2.96	7.04
		3M	2.28		2.62	2.73	1.64	2.01	1.93	1.65	2.97	2.24	2.35
	FP	Vol	8.98	0.5786	2.73	4.82#	2.19	2.34	-	2.72	-	3.54	22.45^
		3M	4.68		3.92^	3.23	2.40	2.38	3.67^	2.03	2.69^	9.79^	6.26^
RMS Cad. Error (RPM)	OA	Vol	6.16	0.0109*	1.60	5.36#	5.90	3.43	5.49^	2.68	7.53^	14.95	9.66^
		3M	1.90		1.20^	3.25	1.88	1.39	1.92^	0.68	2.36^	1.08^	3.35^
	F240	Vol	3.56	0.0336*	1.68	3.94	0.96	0.78	5.49^	1.03	7.53^	1.87	8.74
		3M	1.68		1.16	3.44	0.62	1.00	1.88	0.36	2.42	0.90	3.32
	FP	Vol	12.48	0.0407*	1.25	5.24#	13.06	7.50	-	5.63	-	33.22	21.45^
		3M	3.64		3.09^	2.36	4.01	2.38	2.81^	1.34	1.95^	10.32^	4.52^
% Time in Assist. Mode	F240	Vol	37.92	0.5469	36.68	54.53	10.56	23.24	32.65^	17.39	65.32^	19.83	81.07
		3M	41.74		22.04	80.47	0.28	38.10	68.13	3.35	63.28	11.73	88.30
	FP	Vol	16.17	0.8243	20.34	70.59#	0.00	0.00	-	0.00	-	0.00	22.23^
		3M	22.51		8.64^	46.56	0.00	0.27	41.09^	0.94	56.52^	12.14^	36.47^
% Time in Uncontr. Mode	F240	Vol	55.60	0.3498	59.27	39.61	82.27	72.31	66.03^	73.69	19.12^	72.88	15.23
		3M	50.48		65.40	19.17	75.79	59.86	31.53	84.01	32.42	75.15	11.01
	FP	Vol	13.18	0.0817	65.83	24.01#	0.00	0.00	-	0.98	-	0.00	1.42^
		3M	35.77		36.05^	48.88	11.34	32.44	51.34^	52.36	39.76^	20.93^	28.82^
% Time in Resist. Mode	F240	Vol	6.48	0.6542	4.05	5.86	7.17	4.45	1.32^	8.92	15.55^	7.29	3.70
		3M	7.78		12.57	0.36	23.94	2.04	0.34	12.64	4.29	13.11	0.69
	FP	Vol	70.66	0.1717	13.83	5.40#	100	100	-	99.02	-	100	76.35^
		3M	41.72		55.32^	4.56	88.66	67.28	7.57^	46.70	3.72^	66.93^	34.71^

^= did not complete trial (or portion of the trial).

The last 10 seconds of data was removed since they temporarily stopped pedaling due to instruction confusion.

*Statistical significance for $p < 0.05$, but not significant when adjusted with the Holm-Bonferroni correction for n = 14 comparisons.

OA = overall, F240 = first 240 seconds, FP = final portion, Vol = volitional-only trial, 3M = three mode controller trial.

B. Protocol

Participants completed a warm-up protocol of volitional pedaling at approximately 50 RPM while the resistance of the magnetic trainer was progressively increased. Participant heart rate was measured by a fingertip pulse oximeter. The wheel resistance for subsequent experiments was determined either by the Karvonen formula [38] for desired min/max training heart rate (beginner exercise, 40-50% effort) or by each participant's self report of significant effort that they did not wish to exceed, whichever occurred first.

The remaining protocol consisted of two trials, each five minutes long if fully completed. The first consisted only of volitional pedaling, and the 3M controller was implemented on the second after the participant's heart rate returned to baseline and the participant stated that they were physically ready to continue. During both trials, participants were asked to maintain a cadence within the desired range of 50-55 RPM to the best of their abilities for the first four minutes. For this task, participants were shown a real-time plot of their cadence in comparison to the desired range. Four minutes into each trial, participants were asked to pedal as fast as comfortably possible. Participants were never asked to intentionally pedal below the minimum cadence, but some were incapable of volitionally maintaining a cadence

above the minimum threshold. During the 3M trials, for the first 10 seconds, the cadence approached 50 RPM with the use of the motor. At 10 seconds, the closed-loop motor and FES controller were used when volitional pedaling was below 50 RPM and the motor resisted when volitional pedaling exceeded 55 RPM. Although the goal was five minutes, ultimately, each 3M trial lasted between four and five minutes, depending on patient fatigue and willingness to continue.

The range of crank angles corresponding to the stimulation of each muscle group and activation of the motor within the assistive mode were determined based on the lower thresholds of the torque transfer ratios (see (7)) after measuring the participant's leg lengths and distance to the crank, which were calculated as $\varepsilon_{quad} \in (0.2476, 0.4022)$ for the right and left legs of all participants. The control gains from the FES and motor controllers in (16) and (17), respectively, are selected as follows: $k_{1s} \in (18.75, 43.75)$, $k_{2s} \in (56.25, 131.25)$, $k_{1e} \in (0.375, 1.375)$, $k_{2e} \in (3.75, 4.5)$, $k_a = 0.6$, $k_r = 1$.

C. Results

The root mean square (RMS) cadence error and the standard deviation of the cadence was lower for the 3M trial than the volitional trial for all portions of the trial. Table II indicates

average and standard deviation of the cadence, RMS cadence error, and percent time in each zone for both the volitional and 3M trials for all nine participants. Overall (OA) metrics are separated by the first four minutes (F240), and the final portion (FP) of pedaling to show the effects of the additional volitional effort at the end of each trial. Error is calculated as the difference between the actual cadence and the lower cadence threshold when below the desired range, and the difference between the actual cadence and the upper cadence threshold when above the desired range. Pedaling within the uncontrolled mode/desired cadence range is quantified by an error of zero. Since the participant was asked to pedal with more effort during FP, it was expected that the percent time in each mode would be different between F240 and FP and the overall deviation in cadence was expected to be large. Thus, OA metrics for standard deviation of cadence and percent time in each mode are not included in Table II. OA metrics for average cadence and RMS cadence error are included to demonstrate that, despite varying intensity of volitional contribution, on average the controllers enforced a cadence within the desired uncontrolled range.

Unlike the volitional trials, all nine participants completed the first four minutes of pedaling during the 3M trials, showing the benefit of the 3M control system. However, with more intense effort required after the fourth minute due to additional resistance from the electric motor, Participants 5, 7, and 9 stopped pedaling during the FP of the trial, but before completion, due to fatigue. During the FP of the 3M trial, Participant 8 produced sufficient volitional torque to cause the chain to slip off the motor sprocket. This could be avoided in the future by remounting the idler sprocket to increase the amount of chain wrap around the motor sprocket; however, it was not feasible to do so during the session. Figures 2a-2i depict the cadence from all nine participants during the purely volitional trials. Figures 3a-3i depict the activation of both the motor and FES as the cycle's cadence varies below, within, and above the set cadence thresholds during the 3M trials for all nine participants. Data from the FP of the trial (i.e., when participants were asked to attempt to pedal faster) was not obtained for the volitional trials for Participants 5 or 7 since they were unable to continue cycling on their own past 100 and 120 seconds, respectively. Participant 9 stopped at 250 seconds, shortly after the cue to pedal harder. Participant 2 stopped pedaling momentarily near the end of the volitional trial due to confusion regarding when the trial was supposed to end, so the final 10 seconds were not included in the statistics (but are depicted in Figure 3b).

As seen in Figures 3a-3i, despite each participant's efforts to stay within the desired cadence range, participants experienced all 3Ms, due to a small cadence range relative to the participants' abilities. FES and positive motor current alternated when cadence was below the lower threshold, and the motor provided resistive torques when participants pedaled above target speeds. The average cadence across all nine participants during the 3M trials was within the desired range when calculated over the entire experiment (51.0 RPM), during the first 4 minutes (50.7 RPM), and when the participants were asked to pedal faster at the end of the trial (54.0 RPM). Specifically, Figures 4 and 5 display the change in cadence error and average cadence

during all parts of the volitional and 3M trials. Due to the ability of most participants to volitionally pedal around 50 RPM and since the average was still calculated for participants who fatigued before the trial completed, the overall average cadence did not change significantly from the volitional trials to the 3M trials; however the RMS error (displayed in Figure 6 for all nine subjects) was reduced from the volitional to the 3M trials for all portions of the trials, with p-values of 0.01, 0.03, and 0.04 (not statistically significant when the threshold is adjusted for multiple comparisons) for the OA, F240, and FP of the trials, respectively.

With the data from nine subjects, there is some level of correlation between cycling and walking performance. Table III displays R correlation values for cadence metrics from Table II in comparison to SSWS and FCWS for both the volitional and 3M trials, where an R value equal to 1 would indicate perfect positive correlation, an R value of -1 would indicate perfect negative correlation, and an R value of 0 would indicate no correlation.

V. DISCUSSION

Some participants had difficulty maintaining the minimum desired cadence (e.g., participants depicted in Figures 3b, 3e, 3g, 3i), and thus frequently switched between the assistive and uncontrolled modes, utilizing both FES and the motor. Other participants were able to volitionally reach a desired cadence but had trouble maintaining a steady cadence that remained in the desired range (e.g., Participant 1, Figure 3a), resulting in frequent switching between all 3Ms, but remaining close to the bounds due to the FES and motor controllers. Thus, the percentage of time spent in each of the 3Ms, of which the averages are shown in Figure 7, varied significantly amongst participants (i.e., standard deviations are often larger than the average value), as seen in Table II, indicating that the controller works to maintain a cadence range despite participant ability and various instances of actuators switching, making for an individualized approach. Although it was expected that the assistive and resistive modes would help individuals remain in the uncontrolled mode for a larger percentage of time than when voluntarily pedaling, this was not the case for many of the participants; however, note that this particular statistic is potentially misleading since it does not show how far into each mode the participant pedaled. Figures 3a-3i show that during the 3M trials when participants were pedaling in the assistive or resistive modes, their cadence was not far from the desired, whereas greater deviations occured during the volitional trials. The range of cadence values within one standard deviation of the average is much larger for volitional trials than 3M trials, as shown in Figure 5, as well as larger RMS errors, as shown in Figure 6. Some participants with more strength and coordination were able to volitionally pedal in the desired range for the volitional trial; however, their cadence varied further outside the desired range during volitional trials than with the assistance and resistance of the FES and motor during the 3M trial. Moreover, since Participants 5, 7, and 9 did not complete the volitional trial due to fatigue, the percentage of time spent below the desired range would have
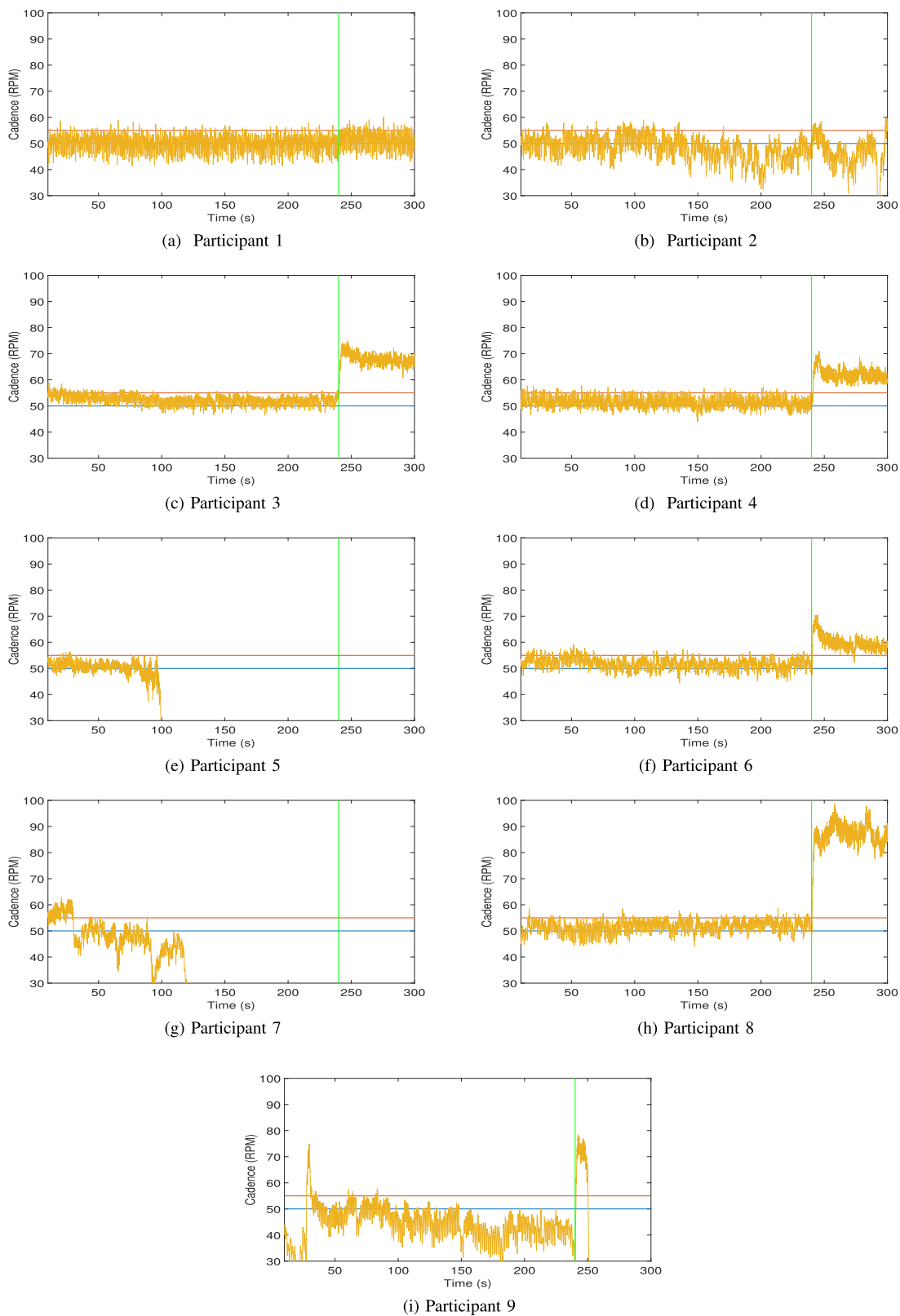
Fig. 2. Cycling cadence in comparison to the desired cadence range during volitional pedaling of target 5 minutes. Upper and lower cadence thresholds are depicted in red and blue and the actual cadence in yellow, respectively, all of which were shown to the participants throughout the trial. Individual results during the volitional-only trials highlight differences in functional performance across participants, and can be compared to the 3M trials depicted in Figs. 3(a)–(i). The vertical green line represents the four minute mark when the participants were asked to pedal at maximum effort.
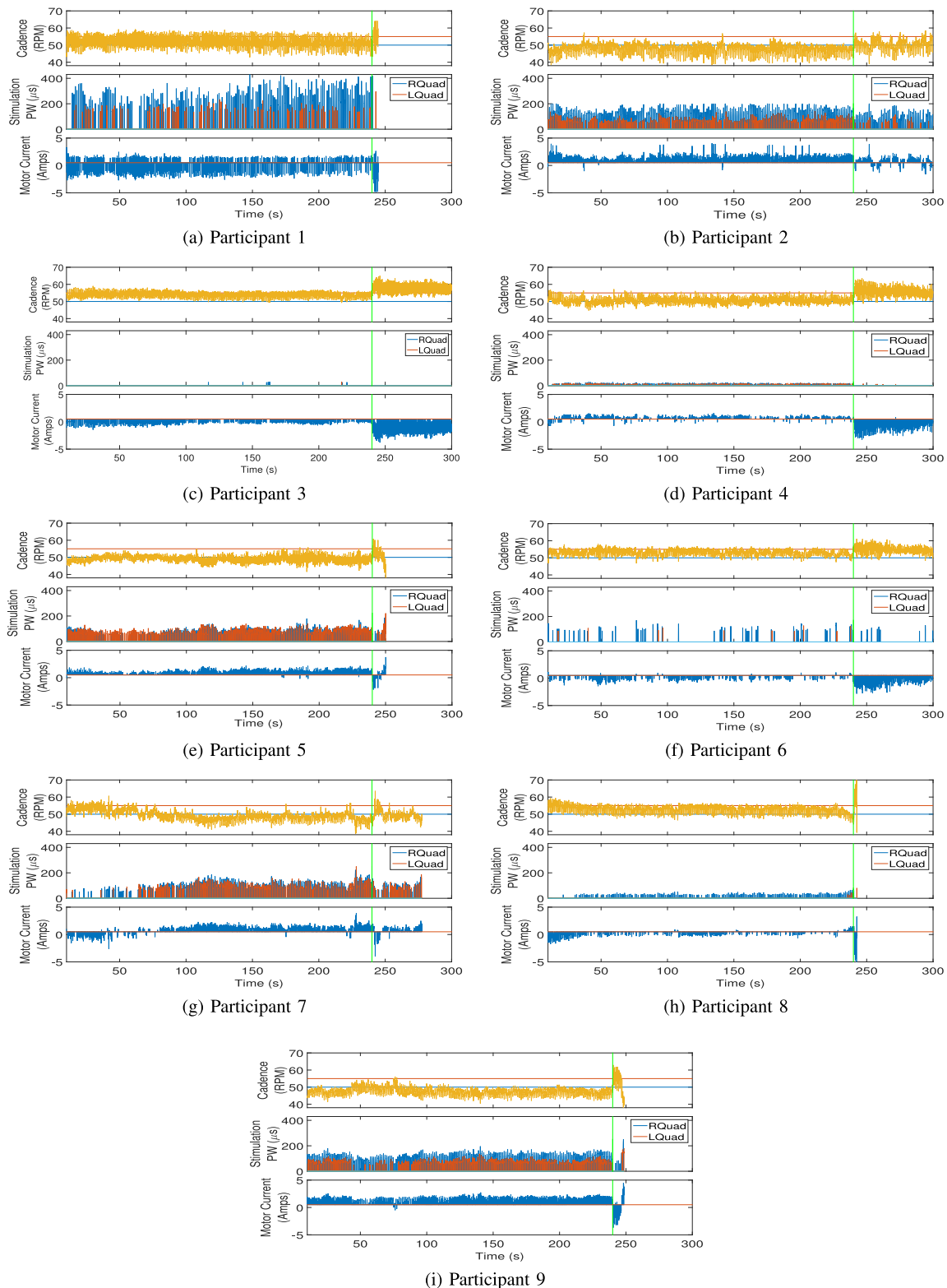
Fig. 3. Cycling cadence (top), stimulation pulsewidth (middle) sent to the right (blue) and left (red) quadriceps, and motor current (bottom) across nine participants. Individual results during the 3M trials highlight how the developed algorithm accommodates for individual differences. The vertical green line represents the four minute mark when the participants were asked to pedal at maximum effort. A current of 0.5 amps (orange line) is used as a feed forward to the motor, so motor current greater than 0.5 amps corresponds to assistance and motor current less than 0.5 amps corresponds to resistance. At steady state, the blue line at 50 RPM and red line at 55 RPM of the cadence plot indicate the selected upper and lower bounds for the uncontrolled mode and the yellow line depicts actual cadence, all of which were shown to the participants throughout the trial. The plots depict the participant attempting to stay within the desired cadence range until minute 4, after which the participant attempts to pedal faster, often transitioning from the uncontrolled mode to the resistive mode. For all participants, when the cadence is below the lower threshold, positive motor input and FES input alternates to assist the participant. When the cadence is above the upper threshold, there is negative motor input.
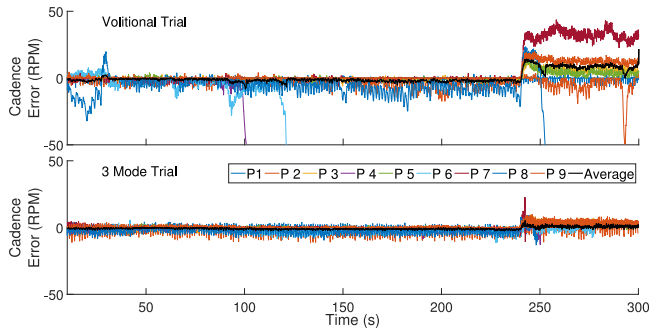
Fig. 4. Cadence error from each participant and average cadence error, for both the volitional (top) and 3M (bottom) trials.
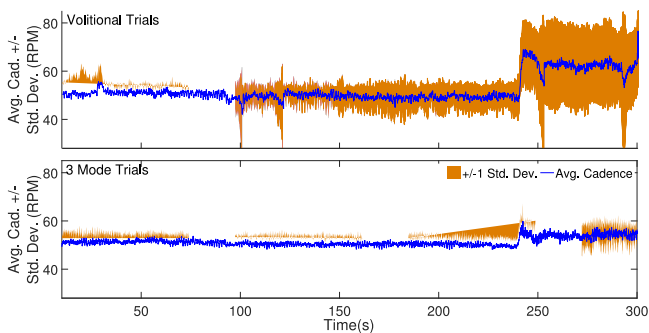

Fig. 5. Cadence averaged over the nine subjects +/- the standard deviation over time for both the volitional (top) and 3M (bottom) trials.
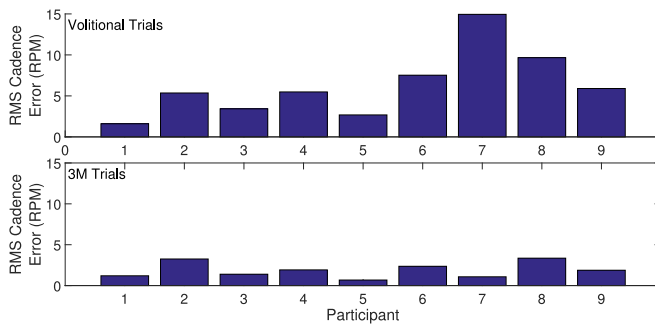

Fig. 6. RMS cadence errors of each of the nine participants for the volitional (top) and 3M (bottom) trials.

likely been significantly more had they continued to try pedaling despite fatigue. Thus, the more noteworthy outcome from the results in Table II is the reduction in standard deviation of the cadence from the volitional pedaling trial to the 3M trial (and consequently, the reduction in RMS error), showing that a more consistent cadence could be maintained compared to volitional pedaling, which is a common goal in rehabilitative cycling [39]. Not all participants experienced a decrease in standard deviation from the FP of the volitional trial to the FP of the 3M trial; however, some participants opted to end trials before completion, rather than slow their cadence, which would've resulted in a larger standard deviation. Such is not reflected in the statistics for the FP. In particular, Participants 4 and 6 would likely had

		SSWS		FCWS	
		Vol.	3M	Vol.	3M
Avg. Cad. (RPM)	OA	0.888	0.850	0.870	0.774
	F240	0.865	0.837	0.785	0.783
	FP	0.493	0.886	0.603	0.858
Cad. SD (RPM)	F240	-0.941	-0.440	-0.861	-0.425
	FP	-0.894	0.140	-0.716	0.292
RMS Cad. Err. (RPM)	OA	-0.038	-0.681	0.072	-0.767
	F240	-0.934	0.384	-0.851	0.453
	FP	0.024	-0.755	0.185	-0.750
% Time in Assist. Mode*	F240	-0.819	-0.864	-0.746	-0.816
	FP	-0.482	-0.833	-0.583	-0.816
% Time in Uncontr. Mode*	F240	0.803	0.865	0.731	0.852
	FP	0.040	-0.408	-0.070	-0.267
% Time in Resist. Mode*	F240	-0.069	0.729	-0.059	0.574
	FP	0.271	0.790	0.396	0.714

*The 3Ms of control do not exist for the volitional-only trial; however, for comparison, the percentage time calculations are based on the same cadence thresholds as in 3M trials.
Participants that did not start the final portion of the volitional trial (indicated by a "-" in Table II) are excluded from the calculation of the R correlation for the FP of the volitional-only trial.
OA = overall, F240 = first 240 seconds, FP =final portion, Vol = volitional-only trial, 3M = three mode controller trial, SSWS = self-selected walking speed, FCWS = fastest comfortable walking speed.
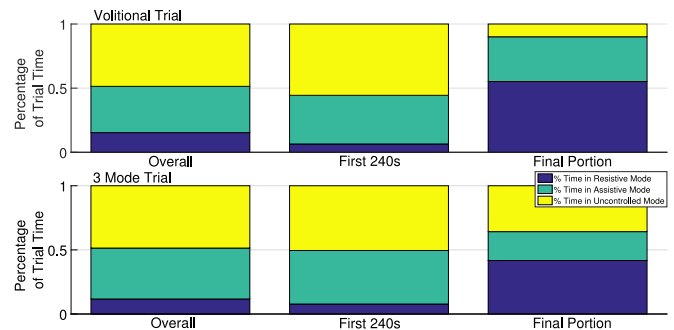

Fig. 7. Average percentage of time in each of the three modes during the OA, F240, and FP portions of both the volitional (top) and 3M (bottom) trials.

larger cadence error and standard deviation during the volitional trials if they had not opted to stop early. Moreover, participants may have exerted more effort than they could maintain for the entire FP, resulting in a larger deviation in cadence than the F240 portion. Standard deviation for the trials OA are not included in Table II since the participants were instructed to purposefully increase their cadence at the four minute mark.

In general, the slower the walker, the slower the cycling cadence in both the volitional and 3M trials, which is evident in the R correlation values between the SSWS and FCWS in the OA and F240 portions, which ranged from 0.774-0.888, as listed in Table III. Both walking speeds correlated more with cadence during the final portion of the 3M trials than volitional-only trials, with respective R correlation values of 0.886 (SSWS) and 0.858 (FCWS) versus 0.493 (SSWS) and 0.603 (FCWS). Thus, it may be concluded that a participant's ability to overcome the

motor resistance better predicts their walking ability than pedaling at a more comfortable cadence does; however, with more than one participant stopping during the final portion of both trials, this statistic does not capture all of the data. Most notably, individuals with the slowest walking speeds (i.e., Participants 7 and 9) were the same participants that did not complete the volitional trial, and were not included in the volitional FP statistics. There is strong evidence of negative correlation between walking speed and the standard deviation of cadence during volitional trials (between -0.941 and -0.716), but dramatically less for 3M trials (between -0.440 and 0.140). Thus, functional ability is an indicator of a person's ability to maintain cycling cadence on their own, but the developed control scheme allowed patients to maintain consistent cadence, no matter their ability, resulting in a low correlation value. The assistance and resistance of the FES and the motor allowed all participants to remain close to the same desired cadence range, unlike volitional pedaling.

Healthy normals can pedal with a small variation in cadence (e.g., within 50-55 RPM) so any deviations show strengths and weaknesses in the participants. However, a higher, lower, wider, or narrower range selected in practice by a physical therapist could significantly alter the amount of time spent in each mode, and thus alter the error values. Regardless, since the motor and FES controllers are exponentially stable in both the assistive and resistive modes, the cadence is mathematically guaranteed to exponentially approach the desired cadence range (see appendix for proof). Even in the case of a patient with complete paralysis, stability can still be guaranteed (set $\tau_{vol} = 0$) and the controller will act as in previous FES studies performed by the authors (e.g., [12]).

VI. CONCLUSION

The novel combined motor and FES control system developed in this paper is designed to enable a cycle rider to maintain cadence within a desired range. With assistive, uncontrolled, and resistive modes, the control system has the potential to advance motorized FES-cycling as a rehabilitation exercise for people with movement disorders. Specifically, FES and a motor can assist those with minimal leg strength or at the onset of fatigue, and the motor can provide resistance to someone who can easily pedal faster than a desired range, for an additional challenge. A Lyapunov-like analysis presented in the appendix proves stability of the controllers for the multi-level switched system, despite unknown disturbances. The development indicates arbitrary switching between the different modes with exponential error convergence despite the rider's capabilities. Experiments performed on nine stroke participants validated the use of the control system in all 3Ms. Despite a wide range of volitional abilities, the participants were able to pedal a recumbant tricycle with average cadences ranging from 47.60 - 54.67 RPM, compared to the desired range of 50-55 RPM. The participants targeted the desired cadence range for the first four minutes, after which they were instructed to pedal with more effort to attempt to overcome the upper threshold.

Future works performed on a decoupled crank cycle would allow assistance and resistance to be applied to each leg

separately so stroke patients cannot compensate for the weakness of their affected side with the strength of their unaffected side. Significant differences in the resulting data of each leg could be used as a metric for rehabilitation improvements. Clinical trials are needed to analyze the effectiveness of the developed control scheme compared to traditional FES-cycling.

APPENDIX
STABILITY ANALYSIS

Let $V_L : \mathbb{R} \rightarrow \mathbb{R}$ be a continuously differentiable, positive definite, common Lyapunov function candidate defined as

$$V_L = \frac{1}{2} M e_1^2, \tag{20}$$

which satisfies the following inequalities:

$$\frac{c_m}{2} e_1^2 \leq V_L \leq \frac{c_M}{2} e_1^2, \tag{21}$$

where c_m and c_M are introduced in Property 1. The use of the common Lyapunov function indicates that arbitrary switching among the different subsystems is possible, as in [40]. Three theorems are presented to cover each possible case where closed-loop control is used.

Theorem 1: When $\dot{q} < \dot{q}_{\underline{d}}$ and $q \in Q_{FES}$, the closed-loop error system in (19) is exponentially stable in the sense that

$$|e_1(t)| \leq \sqrt{\frac{c_M}{c_m}} |e_1(t_n^s)| \exp\left[-\frac{\lambda_s}{2}(t - t_n^s)\right], \tag{22}$$

for all $t \in \left(t_n^s, t_{n+1}^i\right) \forall i \in \{e, p\}$, $\forall n$, where $\lambda_s \in \mathbb{R}_{>0}$ is defined as

$$\lambda_s \triangleq \frac{2}{c_M}\left(c_{b_M} k_{2s} - c_2\right), \tag{23}$$

provided the following sufficient gain conditions are satisfied:

$$k_{1s} > \frac{c_1 + c_{vol}}{c_{b_M}}, \quad k_{2s} > \frac{c_2}{c_{b_M}}, \tag{24}$$

where c_{b_M} is introduced in Property 8, c_1 and c_2 in (15), and k_{2s} and k_{1s} in (16).

Proof: When $\dot{q} < \dot{q}_{\underline{d}}$ and $q \in Q_{FES}$, $e_1 > 0$, $\sigma_a = 1$, and $\sigma_e = 0$ (i.e., the cycle-rider system is controlled by FES in the assistive mode). Due to B_M discontinuously varying over time, the time derivative of (20) exists almost everywhere (a.e.), i.e., for almost all $t \in \left(t_n^s, t_{n+1}^i\right)$, $\forall i \in \{e, p\}$, and after substituting (19), the derivative of (20) can be upper bounded using Properties 7 and 11, Assumption 1, and (15) as

$$\dot{V}_L \overset{\text{a.e.}}{\leq} -\left(c_{b_M} k_{1s} - c_{vol} - c_1\right) e_1 - \left(c_{b_M} k_{2s} - c_2\right) e_1^2, \tag{25}$$

which is negative definite since $e_1 > 0$, provided the gain conditions in (24) are satisfied. Furthermore, (21) can be used to upper bound (25) as

$$\dot{V}_L \leq -\lambda_s V_L, \tag{26}$$

where λ_s denotes a known positive bounding constant, defined in (23). The inequality in (26) can be solved to yield

$$V_L(t) \leq V_L(t_n^s) \exp\left[-\lambda_s(t - t_n^s)\right], \tag{27}$$

for all $t \in \left(t_n^s, t_{n+1}^i\right)$, $\forall i \in \{e, p\}$, $\forall n$. Rewriting (27) using (21) and performing some algebraic manipulation yields exponential convergence of $|e_1(t)|$, as in (22). ∎

Theorem 2: When $\dot{q} < \dot{q}_{\underline{d}}$ and $q \notin Q_{FES}$, the closed-loop error system in (19) is exponentially stable in the sense that

$$|e_1(t)| \leq \sqrt{\frac{c_M}{c_m}} |e_1(t_n^e)| \exp\left[-\frac{\lambda_{e1}}{2}(t - t_n^e)\right], \qquad (28)$$

for all $t \in \left(t_n^e, t_{n+1}^i\right)$, $\forall i \in \{s, p\}$, $\forall n$, where $\lambda_{e1} \in \mathbb{R}_{>0}$ is defined as

$$\lambda_{e1} \triangleq \frac{2}{c_M} \left(c_{b_e} k_a k_{2e} - c_2\right), \qquad (29)$$

provided the following sufficient gain conditions are satisfied:

$$k_{1e} > \frac{c_1 + c_{vol}}{c_{b_e} k_a}, \quad k_{2e} > \frac{c_2}{c_{b_e} k_a}, \qquad (30)$$

where k_{1e} and k_{2e} are introduced in (17), c_1 and c_2 in (15), c_{b_e} in Property 9, and k_a in (18).

Proof: When $\dot{q} < \dot{q}_{\underline{d}}$ and $q \notin Q_{FES}$, $e_1 > 0$, $\sigma_a = 1$, and $\sigma_e = k_a$, but $B_M = 0$ by its definition in (10) and the definition of σ_m. It can be demonstrated that, due to the signum function in (19), the time derivative of (20) exists a.e., i.e., for almost all $t \in \left(t_n^e, t_{n+1}^i\right)$, $\forall i \in \{s, p\}$, and, after substituting (12) and (19), can be upper bounded using Properties 7 and 12, Assumption 1, and (15) as

$$\dot{V}_L \overset{\text{a.e.}}{\leq} -\left(c_{b_e} k_a k_{1e} - c_{vol} - c_1\right) e_1$$
$$- \left(c_{b_e} k_a k_{2e} - c_2\right) e_1^2, \qquad (31)$$

which is negative definite since $e_1 > 0$, provided the control gain conditions in (30) are satisfied. Furthermore, (21) can be used to upper bound (31) as

$$\dot{V}_L \leq -\lambda_{e1} V_L, \qquad (32)$$

where λ_{e1} was defined in (29). The inequality in (32) can be solved to yield

$$V_L(t) \leq V_L(t_n^e) \exp\left[-\lambda_{e1}(t - t_n^e)\right], \qquad (33)$$

for all $t \in \left(t_n^e, t_{n+1}^i\right)$, $\forall i \in \{s, p\}$, $\forall n$. Rewriting (33) using (21), and performing some algebraic manipulation yields exponential convergence of $|e_1(t)|$, as in (28). ∎

Remark: Exponential convergence to $\dot{q}_{\underline{d}}$ throughout the assistive mode (Theorems 1 and 2) is guaranteed in the sense that

$$|e_1(t)| \leq \sqrt{\frac{c_M}{c_m}} |e_1(t_n^i)| \exp\left[-\frac{\lambda_a}{2}(t - t_n^i)\right], \qquad (34)$$

for all $t \in \left(t_n^i, t_{n+1}^p\right)$ $\forall i \in \{e, s\}$, $\forall n$, where $\lambda_a \in \mathbb{R}_{>0}$ is defined as

$$\lambda_a \triangleq \min\{\lambda_s, \lambda_{e1}\}.$$

Since (34) holds for all combinations of σ_e and σ_m while $\sigma_a = 1$, V_L is indeed a common Lyapunov function for switching during the assistive mode.

Theorem 3: When $\dot{q} > \dot{q}_{\overline{d}}$, the closed-loop error system in (19) is exponentially stable in the sense that

$$|e_1(t)| \leq \sqrt{\frac{c_M}{c_m}} \Delta_d \exp\left[-\frac{\lambda_{e2}}{2}(t - t_n^e)\right], \qquad (35)$$

for all $t \in \left(t_n^e, t_{n+1}^i\right)$, $i = p$, $\forall n$, where $\lambda_{e2} \in \mathbb{R}_{>0}$ is defined as

$$\lambda_{e2} \triangleq \frac{2}{c_M} \left(c_{b_e} k_r k_{2e} - c_2\right), \qquad (36)$$

provided the following gain conditions are satisfied:

$$k_{1e} > \frac{c_1 + c_{vol} + c_{B_e} k_{2e} k_r \Delta_d}{c_{b_e} k_r}, \quad k_{2e} > \frac{c_2}{c_{b_e} k_r}, \qquad (37)$$

where c_{b_e} and c_{B_e} were introduced in Property 9, c_{vol} in Assumption 1, k_r in (18), c_1 and c_2 in (15), and Δ_d in (12).

Proof: When $\dot{q} > \dot{q}_{\overline{d}}$, $\sigma_a = 0$, $e_2 < 0$, $e_1 < 0$, and $\sigma_e = k_r$. Due to the signum function in (19), the time derivative of (20) exists a.e., i.e., for almost all $t \in \left(t_n^e, t_{n+1}^p\right)$, and for all n, and, after substituting (12) and (19), can be upper bounded using Properties 7 and 12, Assumption 1, and (15) as

$$\dot{V}_L \overset{\text{a.e.}}{\leq} -\left(c_{b_e} k_r k_{1e} - c_{B_e} k_r k_{2e} \triangle_d - c_1 - c_{vol}\right) |e_1|$$
$$- \left(c_{b_e} k_r k_{2e} - c_2\right) e_1^2, \qquad (38)$$

which is negative definite provided the control gain conditions in (37) are satisfied. Furthermore, (38) can be upper bounded as

$$\dot{V}_L \leq -\lambda_{e2} V_L,$$

and solved to yield

$$V_L(t) \leq V_L(t_n^e) \exp\left[-\lambda_{e2}(t - t_n^e)\right], \qquad (39)$$

for all $t \in \left(t_n^e, t_{n+1}^i\right)$, $i = p$, $\forall n$, where λ_{e2} denotes a known positive bounding constant, and was defined in (36). Rewriting (39) using (21), noting that $|e_1(t_n^e)| = |e_2(t_n^e) - \Delta_d| = \Delta_d$ when $\sigma_a = 0$, and performing algebraic manipulation yields exponential convergence of $|e_1(t)|$ as in (35). ∎

Remark 1: To ensure exponential tracking to the desired cadence range for both the resistive and assistive motor modes, the gain conditions from (30) and (37) are combined as $k_{1e} > \max\left\{\frac{c_1}{c_{b_e} k_a}, \frac{c_1 + c_{vol} + c_{B_e} k_{2e} k_r \Delta_d}{c_{b_e} k_r}\right\}$, $k_{2e} > \max\left\{\frac{c_2}{c_{b_e} k_a}, \frac{c_2}{c_{b_e} k_r}\right\}$.

Since the uncontrolled mode is defined by $0 \leq e_1 \leq \Delta_d$, the error is always bounded in the uncontrolled mode. As described in (22), (28), (35) in Theorems 1–3, and Remark (1), $|e_1|$ decays at an exponential rate in both the assistive and resistive modes. By the definition of e_2 in (12), $|e_2|$ also decays exponentially in the assistive and resistive modes. Therefore, sufficient conditions for overall stability of the two-sided system can be developed based on the exponential time constants λ_s, λ_{e1}, and λ_{e2}. When the system enters the resistive mode, the cadence will exponentially decay back into the uncontrolled mode and when entering the assistive mode, the FES and motor controllers will ensure the cadence exponentially increases back into the uncontrolled range of desired cadence. In this application, where there is a desired cadence range rather than a single desired trajectory,

error convergence to a range of values (Δ_d) is desirable, rather than exponential error convergence to zero.

ACKNOWLEDGMENT

REFERENCES

[1] M. Bélanger *et al.*, "Electrical stimulation: Can it increase muscle strength and reverse osteopenia in spinal cord injured individuals?" *Arch. Phys. Med. Rehabil.*, vol. 81, no. 8, pp. 1090–1098, 2000.

[2] M. M. Rodgers *et al.*, "Musculoskeletal responses of spinal cord injured individuals to functional neuromuscular stimulation-induced knee extension exercise training," *J. Rehabil. Res. Dev.*, vol. 28, no. 4, pp. 19–26, 1991.

[3] L. Popović-Maneski *et al.*, "Assessment of spasticity by a pendulum test in SCI patients who exercise FES cycling or receive only conventional therapy," *IEEE Trans. Neural Syst. Rehabil. Eng.*, vol. 26, no. 1, pp. 181–187, Jan. 2018.

[4] L. Griffin *et al.*, "Functional electrical stimulation cycling improves body composition, metabolic and neural factors in persons with spinal cord injury," *J. Electromyogr. Kinesiol.*, vol. 19, no. 4, pp. 614–622, 2009. Available: http://www.sciencedirect.com/science/article/pii/S105064 1108000436

[5] D. J. Pons, C. L. Vaughan, and G. G. Jaros, "Cycling device powered by the electrically stimulated muscles of paraplegics," *Med. Biol. Eng. Comput.*, vol. 27, no. 1, pp. 1–7, 1989.

[6] L. M. Schutte *et al.*, "Improving the efficacy of electrical stimulation-induced leg cycle ergometry: An analysis based on a dynamic musculoskeletal model," *IEEE Trans. Rehabil. Eng.*, vol. 1, no. 2, pp. 109–125, Jun. 1993.

[7] M. Gföhler *et al.*, "Test bed with force-measuring crank for static and dynamic investigation on cycling by means of functional electrical stimulation," *IEEE Trans. Neural Syst. Rehabil. Eng.*, vol. 9, no. 2, pp. 169–180, Jun. 2001.

[8] J. S. Petrofsky, "New algorithm to control a cycle ergometer using electrical stimulation," *Med. Biol. Eng. Comput.*, vol. 41, no. 1, pp. 18–27, Jan. 2003.

[9] K. J. Hunt *et al.*, "Control strategies for integration of electric motor assist and functional electrical stimulation in paraplegic cycling: Utility for exercise testing and mobile cycling," *IEEE Trans. Neural Syst. Rehabil. Eng.*, vol. 12, no. 1, pp. 89–101, Mar. 2004.

[10] J. S. Petrofsky and J. Smith, "Three-wheel cycle ergometer for use by men and women with paralysis," *Med. Biol. Eng. Comput.*, vol. 30, pp. 364–369, 1992.

[11] T. A. Perkins *et al.*, "Control of leg-powered paraplegic cycling using stimulation of the lumbro-sacral anterior spinal nerve roots," *IEEE Trans. Neural Syst. Rehabil. Eng.*, vol. 10, no. 3, pp. 158–164, Sep. 2002.

[12] M. J. Bellman *et al.*, "Automatic control of cycling induced by functional electrical stimulation with electric motor assistance," *IEEE Trans. Autom. Sci. Eng.*, vol. 14, no. 2, pp. 1225–1234, Apr. 2017.

[13] C. Cousin *et al.*, "Motorized functional electrical stimulation for torque and cadence tracking: A switched Lyapunov approach," in *Proc. IEEE Conf. Decis. Control*, 2017, pp. 5900–5905.

[14] J. Baldi *et al.*, "Muscle atrophy is prevented in patients with acute spinal cord injury using functional electrical stimulation," *Spinal Cord*, vol. 36, no. 7, pp. 463–469, Jul. 1998.

[15] T. Mohr *et al.*, "Increased bone mineral density after prolonged electrically induced cycle training of paralyzed limbs in spinal cord injured man," *Calcif. Tissue Int.*, vol. 61, no. 1, pp. 22–25, 1997.

[16] T. Johnston *et al.*, "Outcomes of a home cycling program using functional electrical stimulation or passive motion for children with spinal cord injury: A case series," *J. Spinal Cord Med.*, vol. 31, no. 2, pp. 215–221, 2008.

[17] S. Ferrante *et al.*, "Cycling induced by functional electrical stimulation improves the muscular strength and the motor control of individuals with post-acute stroke," *Eur. J. Phys. Rehabil. Med.*, vol. 44, no. 2, pp. 159–167, 2008.

[18] S. P. Hooker *et al.*, "Physiologic effects of electrical stimulation leg cycle exercise training in spinal cord injured persons," *Arch. Phys. Med. Rehabil.*, vol. 73, no. 5, pp. 470–476, 1992.

[19] C. L. Sadowsky *et al.*, "Lower extremity functional electrical stimulation cycling promotes physical and functional recovery in chronic spinal cord injury," *J. Spinal Cord Med.*, vol. 36, no. 6, pp. 623–631, 2013.

[20] D. Kuhn, V. Leichtfried, and W. Schobersberger, "Four weeks of functional electrical stimulated cycling after spinal cord injury: A clinical study," *Int. J. Rehabil. Res.*, vol. 37, pp. 243–250, Mar. 2014.

[21] A. T. Harrington, C. G. A. McRae, and S. C. K. Lee, "Evaluation of functional electrical stimulation to assist cycling in four adolescents with spastic cerebral palsy," *J. Pediatr.*, vol. 2012, pp. 1–11, 2012.

[22] N. Makowski *et al.*, "Interaction of post-stroke voluntary effort and functional neuromuscular electrical stimulation," *J Rehabil. Res. Dev.*, vol. 50, no. 1, pp. 85–98, Jan. 2013.

[23] A. U. Pehlivan, F. Sergi, and M. K. O'Malley, "A subject-adaptive controller for wrist robotic rehabilitation," *IEEE Trans. Mechatron.*, vol. 20, no. 3, pp. 1338–1350, Aug. 2015.

[24] A. Bettini *et al.*, "Vision-assisted control for manipulation using virtual fixtures," *IEEE Trans. Robot.*, vol. 20, no. 6, pp. 953–966, Dec. 2004.

[25] M. Coad *et al.*, "Training in divergent and convergent force fields during 6-DOF teleoperation with a robot-assisted surgical system," in *Proc. IEEE World Haptics Conf.*, Jun. 2017, pp. 195–200.

[26] I. Nisky, M. Hsieh, and A. Okamura, "Uncontrolled manifold analysis of arm joint angle variability during robotic teleoperation and freehand movement of surgeons and novices," *IEEE Trans. Biomed. Eng.*, vol. 61, no. 12, pp. 2869–2881, Dec. 2014.

[27] S. Srivastava *et al.*, "Robotic assist-as-needed as an alternative to therapist-assisted gait rehabilitation," *Int. J. Phys. Med. Rehabil.*, vol. 4, no. 5, Oct. 2016, Art. no. 370.

[28] S. Srivastava *et al.*, "Assist-as-needed robot-aided gait training improve walking function in individuals following stroke," *IEEE Trans. Neural Syst. Rehabil. Eng.*, vol. 23, no. 6, pp. 956–963, Nov. 2015.

[29] C. Krishnan *et al.*, "Reducing robotic guidance during robot-assisted gait training improve gait function: A case report on a stroke survivor," *Arch. Phys. Med. Rehabil.*, vol. 94, no. 6, pp. 1202–1206, Jun. 2013.

[30] C. Krishnan *et al.*, "Active robotic training improve locomotor function in a stroke survivor," *J. Neuroeng. Rehabil.*, vol. 9, no. 1, 2012, Art. no. 57.

[31] M. J. Bellman *et al.*, "Stationary cycling induced by switched functional electrical stimulation control," in *Proc. Amer. Control Conf.*, 2014, pp. 4802–4809.

[32] M. J. Bellman *et al.*, "Cadence control of stationary cycling induced by switched functional electrical stimulation control," in *Proc. IEEE Conf. Decis. Control*, 2014.

[33] M. J. Bellman *et al.*, "Switched control of cadence during stationary cycling induced by functional electrical stimulation," *IEEE Trans. Neural Syst. Rehabil. Eng.*, vol. 24, no. 12, pp. 1373–1383, Dec. 2016.

[34] M. M. Ouellette *et al.*, "High-intensity resistance training improves muscle strength, self-reported function, and disability in long-term stroke survivors," *Stroke*, vol. 35, no. 6, pp. 1404–1409, 2004.

[35] C. Rouse *et al.*, "Cadence tracking for switched FES cycling combined with voluntary pedaling and motor resistance," in *Proc. Amer. Control Conf.*, 2018, pp. 4558–4563.

[36] T. Yan, C. W. Y. Hui-Chan, and L. S. W. Li, "Functional electrical stimulation improves motor recovery of the lower extremity and walking ability of subjects with first acute stroke: A randomized placebo-controlled trial," *Stroke*, vol. 36, no. 1, pp. 80–85, 2005. [Online]. Available: http://stroke.ahajournals.org/cgi/content/abstract/36/1/80

[37] S. Kim *et al.*, "Effects of stationary cycling exercise on the balance and gait abilities of chronic stroke patients," *J. Phys. Therapy Sci.*, vol. 27, no. 11, pp. 3529–3531, Nov. 2015.

[38] M. Karvonen, E. Kentale, and O. Mustala, "The effects of training on heart rate; a longitudinal study," *Ann. Med. Exp. Biol. Fenn.*, vol. 35, no. 3, pp. 307–315, 1957.

[39] A. Ridgel *et al.*, "Variability in cadence during force cycling predict motor improvement in individuals with Parkinson's disease," *IEEE Trans. Neural Syst. Rehabil. Eng.*, vol. 21, no. 13, pp. 481–489, May 2013.

[40] D. Liberzon, *Switching in Systems and Control*. Cambridge, MA, USA: Birkhauser, 2003.